Applied Energy 364 (2024) 123145

Contents lists available at ScienceDirect

Applied Energy

journal homepage: www.elsevier.com/locate/apenergy

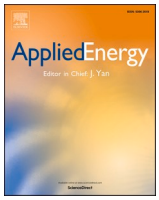

Kinetic energy harvesting for enhancing sustainability of refrigerated transportation

Angelo Maiorino, Fabio Petruzziello *, Arcangelo Grilletto, Ciro Aprea

Department of Industrial Engineering, University of Salerno, Via Giovanni Paolo II 132, 84084 Fisciano, SA, Italy

HIGHLIGHTS

- A KERS for powering a commercial transport refrigeration system is proposed.
- The dynamic performances of a KERS are evaluated through numerical modelling.
- Performance evaluation is based on a real single-delivery mission.
- The real conversion efficiencies are considered.
- The electrical energy demand coverage ratio and subsequent benefits are assessed.

ARTICLE INFO

Keywords:
Refrigerated transport
Sustainability
Numerical modelling
Carbon footprint
Fuel savings

ABSTRACT

The industry of temperature-controlled transportation has shown significant growth in recent years, and this growth is expected to continue in the future. As the sector expands, it's crucial to focus on reducing energy consumption and greenhouse gas emissions related to transport refrigeration systems to meet the planned decarbonization goals. In this study, the energy and environmental benefits of implementing an electric Kinetic Energy Recovery System (KERS) on a refrigerated light-duty commercial van, equipped with a vapor compression refrigeration (VCR) system, are assessed by means of dynamic simulation. The KERS considered involves a $LiFePO_4$ battery as electricity storage system, a brushless motor-generator unit and a hybrid inverter able to both charge the battery and power the refrigeration system. For each component of the system, i.e. the engine, the alternator, the transmission system and the KERS, the real efficiencies have been considered. The dynamic behaviour of the KERS is simulated by using data obtained by performing a real urban single-delivery 40 km mission, during which the vehicle operating conditions, as well as the electricity demand of the refrigeration system, have been measured. The estimation of the potential benefits of the proposed solution has been performed by comparing the electricity produced by the KERS (and available for use) and the measured energy demand of the refrigeration system.

The results have shown that the electricity available for use could cover more than 47% of the total electricity demand. This means that nearly half of the primary energy/fuel consumption can be saved by employing a KERS in refrigerated-light duty vehicles. In particular, emissions savings ranging between 9 and 13 $g_{CO2,e}$ and cost savings between 0.4 and 0.7 c€ per kilometer travelled can be achieved, resulting in an average payback period of 8 years. In addition, when considering the entire useful life of a refrigerated van equal to 10 years, CO2,e savings of 4515–6710 $kg_{CO2,e}$ are obtained.

The low complexity of the proposed system and the availability of the components on the market, together with the results obtained by simulation, make using KERS in refrigerated transport a promising solution throughout the decarbonization of the refrigerated transport sector.

1. Introduction

The air conditioning and refrigeration sectors are major energy

* Corresponding author.
E-mail address: fpetruzziello@unisa.it (F. Petruzziello).

https://doi.org/10.1016/j.apenergy.2024.123145
Received 11 February 2024; Received in revised form 25 March 2024; Accepted 30 March 2024
Available online 4 April 2024

Nomenclature

Symbols

a	Vehicle acceleration
A_f	Frontal surface area of the vehicle
c	Unit
C_r	Rolling resistance coefficient
C_x	Aerodynamic drag coefficient of the vehicle
E	Energy
F	Force
f_{KERS}	Electricity demand coverage ratio
g	Gravitational acceleration
I	MGU rotor inertia
i	Current
k	Windage losses constant of the MGU
m_{fuel}	Fuel consumption
m_v	Vehicle mass
P	Power
P_{el}	Active electrical power
R	Resistive losses constant of the MGU
S_{el}	Apparent electrical power
t	Time
T	Torque
T_f	Constant friction torque of the MGU
T_{stall}	Stall torque of the MGU
V	Voltage
v	Vehicle speed

Greek symbols

α	Angular acceleration of the MGU
α_{fuel}	Emission factor of the fuel
η	Efficiency
ϑ	Street angle
ρ_{air}	Air density
ω	Angular speed of the MGU

Subscripts

aer	Aerodynamic
alt	Alternator
available	Available to power the VCR unit
B	Battery
BL	Battery-Limited
br	Braking
D	Differential gear
en	Engine
fuel	fuel
G	MGU Gear
I	Inertia
inv,ch	Inverter in charge mode
inv,dis	Inverter in discharge mode
KERS	KERS
min	minimum
max	Maximum
MGU	MGU
nom	Nominal or average
P	Active electrical energy
ref	refrigeration/refrigeration unit
roll	rolling
t	transmission
tot	Total
traction	Traction
W	Weight

Acronyms

AC	Alternating Current
CAGR	Compound Annual Growth Rate
COP	Coefficient Of Performance
DC	Direct Current
FS	Fuel Saving
KERS	Kinetic Energy Recovery System
LHV	Lower Heating Value of the fuel
MGU	Motor-Generator-Unit
OBD	On-Board Diagnostic
PES	Primary Energy Saving
VCR	Vapor Compression Refrigeration

consumers globally, accounting for around 20% of the world's electricity [1]. The cold chain is crucial for preserving temperature-sensitive products through production, packaging, storage, transportation, and preservation stages. Vapor Compression Refrigeration (VCR) systems dominate these sectors, representing about 80% of the market share [2]. These systems utilize refrigerants that absorb and release heat through phase changes. The main component, the compressor, consumes the most energy. Inefficient energy use in VCR systems contributes to global warming, primarily through indirect emissions from energy production and direct emissions from refrigerant leakages [3,4]. Efforts to reduce VCR systems' energy consumption include technological modifications and the use of renewable energy sources. Innovations aim to improve energy consumption and decrease emissions [5–12]. Refrigerated transport is a critical part of the cold chain, significantly impacting consumption and emissions.

According to UNEP [13], in 2010 there were around 4 million vehicles in circulation in the world, including vans (40%), large trucks (30%), semi-trailers or trailers (30%). The total number of refrigerated vehicles worldwide is expected to reach 15.5 million by 2025 [14]. The refrigerated transport market is expected to grow from $USD 113.4 billion in 2022 to $USD 160.7 billion by 2027 at a CAGR of 7.2% [15].

Most refrigerated vehicles use VCR systems powered by internal combustion engines. Challenges include variability in working conditions and high energy consumption [16,17]. Efforts to reduce emissions from refrigerated transport include alternative refrigeration systems, such as absorption/adsorption systems, CO_2-based systems, and passive cooling methods. Fuel cells present a promising alternative but require further development due to high costs [18–20]. Sustainable growth in the refrigerated transport industry requires addressing scientific and technical challenges, including vehicle and refrigeration equipment design and optimization. The European Commission aims for a 40% decrease in greenhouse gas emissions by 2030 and advocates for hybridization and electrification of all sectors to achieve climate targets [21,22]. The transition to a more sustainable model based on energy efficiency and renewable sources requires overcoming the traditional fossil fuel-based energy model [23]. Efforts include research on cleaner fuels, design and optimization of electric and hybrid vehicles, and energy management strategies [24–26].All these research topics aim to reduce the automotive sector's environmental impact. Another interesting possibility for reducing fuel consumption and emissions is represented by kinetic energy recovery systems (KERS), which can partially recover the energy that is usually dissipated during the braking and deceleration phases. The energy recovered can then be stored in a storage system.

Various types of KERS have been proposed and optimized in the literature, mainly based on the specific energy storage systems they employ. Unlike electric and hybrid electric vehicles, internal combustion engine vehicles do not have the necessary equipment, such as a

generator, electric motor, and battery with sufficient capacity and power, to convert kinetic energy into electricity and reuse it for propulsion. For this reason, most of the KERS successfully tested for internal combustion vehicles are based on mechanical and hydraulic energy storage devices. Springs and elastomers, for example, can be employed to store mechanical energy obtainable by deforming a metallic spring or an elastomer. In this case, a fuel economy improvement of 15% has been estimated by simulation [27]. In the case of pneumatic and hydraulic KERS, fuel efficiency improvements of 25% and 35%, respectively, have been found [28]. Another mechanical KERS is represented by the flywheel one, which can store kinetic energy into the rotational energy of a flywheel. This type of KERS can decrease fuel consumption by up to 20% [29].

The only example of KERS employing electricity storage is the alternator-control KERS, which has been introduced in the automotive sector by some car manufacturers, such as BMW Efficient Dynamics [30]. In this case, the alternator output is increased during braking phases, and the energy is stored in the vehicle's battery to reduce the electricity demand of auxiliaries during the acceleration phases. However, such a system can provide only a slight reduction in fuel consumption, ranging from 1% to 5% [29].

Most of the studies in the literature focus on using KERSs for traction applications, especially for electric and hybrid electric vehicles, to increase the cruise range of the batteries. Only few studies involving the use of KERS to power the air conditioning unit of electric vehicles can be found in the literature [31,32]. Results have shown a slight decrease in energy consumption, increasing the battery cruise range (about 3%).

Ref [33] provides additional information regarding regenerative braking systems, including energy storage systems and control strategies.

The development of electromechanical and electrical power units is relevant for vehicles operating under frequent acceleration and braking conditions, which are typical of urban refrigerated transport.

Notably, there are no studies in the scientific literature in which electrical energy produced by KERS is used to power the compressor of a refrigeration unit in a refrigerated van.

According to the scientific literature, Transport Refrigeration Units (TRUs) are responsible for about 15–25% of the vehicle's total fuel consumption [34] and about 11% according to experimental tests performed in the specific case of a light-duty commercial refrigerated van, as reported in Appendix A. As can be clearly noted, the energy/fuel savings attainable by employing a KERS are comparable to TRUs' impact on energy/fuel consumption.

Starting from this consideration and considering the results achievable by hybridizing refrigerated vans [35], this work examines the potential of implementing an electric KERS in a commercial refrigerated van that uses an all-electric VCR system operating with R-452 A. In this configuration, the three-phase rotary compressor is powered by an inverter, which can be supplied by the power grid (230 V, single phase) when the vehicle is turned off. When the thermal engine is running, it mechanically drives an auxiliary alternator through a pulley and belt transmission, supplying electricity to the inverter. In particular, the energy recovered during braking phases using a generator can be stored in a battery after the required AC/DC conversion and used to power the refrigeration unit when needed. Starting from what the scientific literature offers, a KERS model [36] has been adapted to a specific Motor-Generator Unit (MGU) and used to estimate the attainable cost and emission savings. These results have been obtained by comparing the electrical energy produced by the KERS (and can be drawn from the battery) to the actual energy demand of the VCR system measured during a real single-delivery mission. The evaluation of the payback period related to the implementation of the proposed solution follows. It needs to be pointed out that all the components are assumed not to deteriorate over time, since this is a first preliminary study. Surely this aspect must be taken into account in future works, especially when considering the battery, which performance and lifespan may strongly vary over time [37].

The cold chain (and the refrigeration sector in general) needs to be improved in order to meet the decarbonization goals. The scientific community has given significant attention to achieving sustainability in stationary refrigeration systems, but more needs to be done to ensure the sustainability of refrigerated transportation. The proposal of using an electric KERS to power the VCR unit for a refrigerated vehicle is a novel solution that has not been mentioned in the literature before. This approach could reduce fuel consumption for refrigeration in internal combustion refrigerated vehicles meeting the decarbonization goals and making refrigerated transportation sustainable.

2. Reference system and model description

A solution to reduce fuel consumption and CO_2 emissions related to the operation of a VCR system serving a refrigerated light-duty vehicle is to explore the use of an electric Kinetic Energy Recovery System (KERS), intending to decrease the reliance on the thermal engine. In this section, the authors provide a comprehensive overview of the reference system, detailing the various steps involved in converting energy produced by the KERS to power the refrigeration unit. In order to estimate the achievable benefits, a mathematical model based on that reported in [36] is applied.

The schematic of the overall system is shown in Fig. 1, where the additional KERS system is highlighted.

A $LiFePO_4$ battery is considered as storage for the electricity produced by means of a Motor-Generator Unit (MGU), which is mechanically connected to the engine drive shaft via a fixed-ratio gear transmission. The authors focused on brushless motors because of their advantageous features, such as high efficiency, fast dynamic response, greater power density, and longer lifespan compared to traditional brushed motors. In particular, a three-phase permanent magnet synchronous motor has been selected.

A $LiFePO_4$ (lithium-iron-phosphate - LFP) battery has been selected for this study due to its high-temperature stability and eco-friendliness. In addition, the main components of LFP batteries, such as Fe and P, are abundant and cost-effective natural resources compared to other types of lithium-ion batteries. Moreover, the stable olivine crystal structure of LFP is maintained by strong Fe—O and P—O bonds, allowing for safe handling and a long service life [38]. In addition to safety, economic and environmental benefits, it is important to note that the automotive industry is focusing on manufacturing and marketing hybrid and electric vehicles that use lithium batteries. This type of battery exhibits high power and energy density (same capacity but lower weight and size, meaning a slighter effect on fuel consumption), no memory effects and excellent storage/recharge capabilities [39]. Due to these considerations, $LiFePO_4$ batteries represent the ideal choice for the application of the proposed system to every type of vehicle (current and next-future).

Since the generator is able to produce three-phase electrical power, a conversion into DC power to charge the battery is needed. For this purpose, the proposed system requires a hybrid inverter to regulate the power transfer between the MGU and the battery. This device comprises both an AC/DC converter to convert the AC current provided by the MGU into DC current, and a step-up/step-down DC/DC converter to adjust the voltage to the needed value. During the braking or deceleration process, the MGU serves as a generator and aids in reducing the vehicle's speed by transferring a portion of the vehicle's kinetic energy to the battery via the hybrid inverter. The latter adjusts the voltage of the MGU drive to match that of the battery and regulates the electric current flowing to the battery based on the power received by the MGU. When the refrigeration system is running, the hybrid inverter converts the DC power provided by the battery into AC.

2.1. KERS model

Considering the energy produced by the KERS and used to charge the

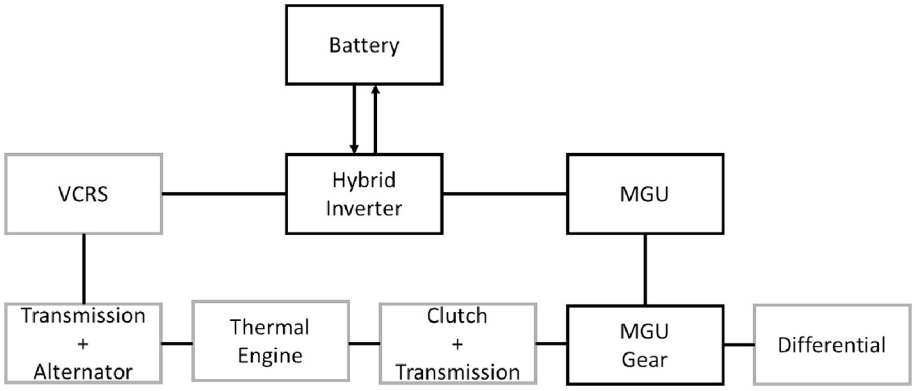

Fig. 1. Schematics of the proposed hybrid refrigerated van.

battery, the power flow follows the red blocks shown in Fig. 1, from the wheels to the battery. The whole conversion process involves several steps, as described in this subsection.

The first step is the evaluation of the braking power, which represents the input of the KERS model. To this purpose, all the forces acting on the longitudinal dynamics of the refrigerated vehicle are taken into account (Eq. (1)).

$$F_{traction}(t) - F_{br}(t) - [F_{aer}(t) + F_{roll}(t) + F_w(t)] = F_I(t) \tag{1}$$

where $F_{traction}$ and F_{br} are the traction and braking forces acting on the vehicle, respectively. F_{aer}, F_{roll} and F_w are the resistances due to the aerodynamic drag, the rolling friction and the weight of the vehicle, respectively. The right-hand side of the equation is represented by the inertia force (F_I), given by the product between the vehicle's total mass (m_v), including the KERS, the inverter and the battery pack, and its acceleration (a_v). The resistance terms F_{aer}, F_{roll} and F_w can be evaluated as follows.

$$F_{aer}(t) = \frac{1}{2} \bullet C_x \bullet \rho_{air} \bullet A_f \bullet v^2(t) \tag{2}$$

$$F_{roll}(t) = C_r \bullet m_v \bullet g \bullet sin[\theta(t)] \tag{3}$$

$$F_w(t) = m_v \bullet g \bullet cos[\theta(t)] \tag{4}$$

where:

- C_x is the aerodynamic drag coefficient of the vehicle;
- ρ_{air} is the air density;
- A_f is the frontal surface area of the vehicle;
- v is the vehicle's speed;
- C_r is the rolling friction coefficient;
- g is the gravitational acceleration;
- ϑ is the street angle.

During braking phases, the traction force is equal to zero. The braking power can be evaluated by multiplying Eq. (1) by the van's speed $v_v(t)$, as shown in Eq. (5).

$$P_{br}(t) = \left[m_v \bullet a_v(t) - \frac{1}{2} \bullet C_x \bullet \rho_{air} \bullet A_f \bullet v^2(t) - C_r \bullet m_v \bullet g \bullet sin[\theta(t)] - m_v \bullet g \bullet cos[\theta(t)] \right] \bullet v(t) \tag{5}$$

It is worth noting that Eq. (9) involves both braking and deceleration phases, which both can be exploited to produce electricity by means of the KERS. However, the power that can be converted by the KERS is limited by several factors, as described in [36], which considers the use of an electric KERS for traction applications, so the MGU acts as a generator in deceleration phases and as a motor in acceleration ones. The second step is therefore given by the identification of such limitations, so that the power produced by the MGU can be evaluated by means of Eq. (6).

$$P_{MGU}(t) = V_{MGU} \bullet i_{MGU}(t) = T_{MGU}(t) \bullet \omega(t) - R \bullet i^2_{MGU}(t) - T_F \bullet \omega(t) - k \bullet \omega^3(t) - I \bullet \alpha(t) \bullet \omega(t) \tag{6}$$

where P_{MGU} is the power output of the KERS, given by the product between the MGU voltage (V_{MGU}) and the current (i_{MGU}). In case of zero losses, the P_{MGU} should be also equal to the product between the torque T_{MGU} and the rotation speed ω. R and TF are coefficients related, respectively, to resistive (proportional to the square value of the current i_{MGU}) and friction (proportional to the angular speed) losses, while k-term is used to consider a third loss which is proportional to the cube of the angular velocity, representing windage losses. These parameters have been obtained by tuning the model with the experimental data provided by the manufacturer. The last term in the right-hand side is related to the inertia of the rotor of the MGU, given by the product between the rotational inertia (I) and the angular acceleration (α).

The MGU angular speed can be evaluated as a function of the vehicle's speed and the wheel radius R_w, as shown in Eq. (7).

$$\omega(t) = \frac{v(t)}{R_w} \bullet \tau_D \bullet \tau_G \tag{7}$$

where τ_D and τ_G are the differential and MGU gear transmission ratio, respectively. The angular acceleration (α) can be therefore evaluated as the first order derivative of the angular speed.

The first one is given by the stall torque (T_{stall}) of the MGU, which is the maximum torque that the generator is able to receive as input. T_{stall} is a characteristic of the specific MGU considered.

The second limitation is given by the maximum allowed MGU current ($i_{MGU,max}$), which depends on the specific motor-generator. Substituting the $i_{MGU,max}$ in the torque equation, which can be obtained by dividing both members of Eq. (6) by ω(t), the current limited torque ($T_{MGU,CL}$) can be evaluated (Eq. (8)).

$$T_{MGU,CL}(t) = \frac{V_{MGU} \bullet i_{MGU,max}}{\omega(t)} - \frac{R \bullet i^2_{MGU,max}}{\omega(t)} - T_F - k \bullet \omega^2(t) - I \bullet \alpha(t) \tag{8}$$

The last constraints is related to the maximum current that the battery can receive as input ($i_{MGU,BL}$). The evaluation of this limited torque ($T_{MGU,BL}$) can be performed by solving Eq. (9), which can be obtained by considering $i_{MGU,BL}$ in the torque equation.

$$T_{MGU,BL}(t) = \frac{V_{MGU} \bullet i_{MGU,BL}}{\omega(t)} - \frac{R \bullet i^2_{MGU,BL}}{\omega(t)} - T_F - k \bullet \omega^2(t) - I \bullet \alpha(t) \tag{9}$$

The maximum charge current allowed by the battery ($i_{MGU,BL}$) can be obtained by solving Eq. (10).

$$i_{MGU,BL} = \frac{P_{B,max}}{V_{MGU} \bullet \eta_{inv,charge}} \tag{10}$$

where $P_{B,max}$ and $\eta_{inv,ch}$ are the maximum charge power and the efficiency in charge mode of the hybrid inverter, respectively.

Considering these three limits, the maximum torque received by the MGU can be evaluated at each time instant as the minimum value between the three constraints, as reported in Eq. (11).

$$T_{MGU,max}(t) = min\left(T_{stall}; T_{MGU,CL}; T_{MGU,BL}\right) \tag{11}$$

The input power to the MGU $P_{MGU,in}(t)$ is therefore given by the minimum value between the braking power multiplied by the efficiencies of the differential (η_D) and the gear transmissions (η_G), and the maximum allowed value involving the three above-described limitations.

$$P_{MGU,in}(t) = min\left(P_{br}(t) \bullet \eta_D \bullet \eta_G ; T_{MGU,max}(t) \bullet \omega(t)\right) \tag{12}$$

The output power of the MGU and therefore the input power to the hybrid inverter, can be evaluated by considering the MGU efficiency (η_{MGU}), which is a function of the input torque and the rotational speed $\omega(t)$. The evaluation of the η_{MGU}) has been performed by implementing in the model the characteristic surface of the MGU considered.

The $P_{MGU,out}(t)$, and consequently the inverter input power $P_{inv,in}(t)$, can be evaluated by solving Eq. (13).

$$P_{MGU,out}(t) = P_{MGU,in}(t) \bullet \eta_{MGU}\left(T_{MGU,in}(t), \omega(t)\right) \tag{13}$$

As previously described, the electricity produced by the KERS (three-phase) must undergo the AC/DC conversion by means of the inverter, characterized by a charge efficiency $\eta_{inv,ch}$. Therefore, the input power to the battery ($P_{B,in}$) can be evaluated by means of Eq. (14).

$$P_B(t) = P_{MGU,out}(t) \bullet \eta_{inv,ch} \tag{14}$$

The model is able to provide the input power to the battery at each instant given the specific driving cycle considered since it gives the van's speed and acceleration as input. The total electricity stored in the battery can, therefore, be evaluated as follows.

$$E_B = \int_{t_0}^{t_{end}} P_B(t) \bullet dt \tag{15}$$

2.2. Data collection

This work aims to evaluate the potential savings, both in environmental and economic terms, attainable by using an electric KERS to power a VCR system in a refrigerated transport application. To this aim, a real single-delivery mission has been performed. In this work, no standardized driving cycles (e.g. NEDC or WLTP driving cycles) have been considered, since they cannot fully represent real-world acceleration or deceleration phases due to casual traffic conditions in urban paths. The delivery mission performed involves a first part in which the VCR unit is running and a second one in which the van is returning to the depot, so the refrigeration unit is not working.

Table 1
Characteristics of the delivery mission.

Mission	Distance	39.6 km
	Duration	83 min
Delivery part	Distance	20 km
	Duration	43 min
Return to depot	Distance	19.6 km
	Duration	40 min
Difference in elevation	310 m	
Set-point temperature	−10 °C	
External temperature	24 °C	

The characteristics of the specific path are shown in Table 1 and Fig. 2.

The choice of the starting and delivery points, together with the whole path, have been chosen in order to obtain a driving cycle including climbs, descents, straight sections and curves, representing a typical road travel path in Italy.

The van's speed during the delivery mission has been obtained by means of an OBD (On-Board Diagnostic) scanner, which is able to provide real time engine operating data with a sampling time of 0.25 s. The van's speed during the travel is a key parameter, since it allows to calculate the MGU angular speed and acceleration, but also the vehicle's acceleration, which affects the braking power (Eq. (9)). The van's speed during the path is shown in Fig. 3.

During the VCR unit operation, the electrical energy consumption has been measured by means of an energy meter with a declared accuracy of ±0.7% of measured value. In particular, both active and apparent electrical power (P_{el} and S_{el}, respectively) and energy (E_P and E_S, respectively) have been measured. The reason is that the battery, which is charged by means of the MGU in the considered setup, provides DC power to be converted into AC power, specifically apparent power.

The electrical energy required by the refrigeration unit can be therefore calculated by integrating electrical power in time (Eqs. 16a and 16b for active and apparent electrical energy, respectively).

$$E_P = \int P_{el}\, dt \tag{16a}$$

$$E_S = \int S_{el}\, dt \tag{16b}$$

The calculation of E_S allows, therefore, the estimation of the amount

Fig. 2. Real single-delivery mission path.

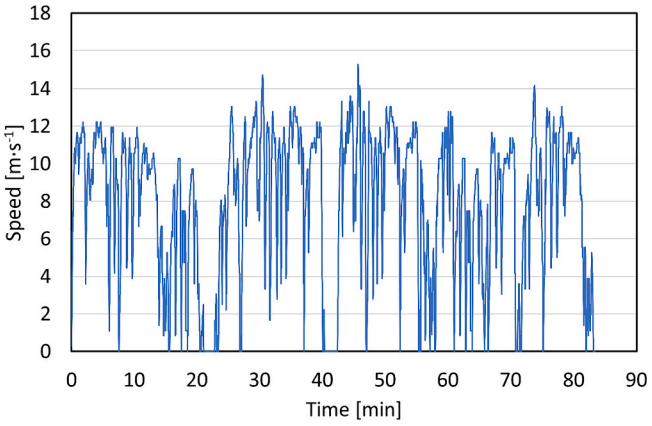

Fig. 3. Measured driving cycle.

of electrical energy demand that can be covered by the energy produced by the KERS and made available by the battery after DC/AC conversion.

Together with electrical energy, the temperature inside the cold chamber and the external one have also been measured by means of two four-wire Pt100 having an accuracy of ±0.15 °C. These measurements have been performed in order to evaluate the correct operation of the refrigeration system (i.e. minimum, maximum and mean temperature inside the cold room). The external temperature has also been measured because it deeply affects the VCR system performance in terms of cooling capacity and energy consumption.

2.3. Energy, environmental and economic performance parameters

In this subsection, all the parameters used to estimate the performance of the proposed system in terms of energy, economic and environmental savings are described.

An electricity demand coverage ratio (f_{KERS}) can be evaluated as the ratio between the electricity produced by the KERS which is actually available ($E_{available}$) for the compressor supply and the apparent electrical energy required by the VCR unit (Eq. (17)). The energy stored in the battery (E_B) must undergo DC/AC conversion to be used to power the VCR system, so the discharge efficiency of the inverter ($\eta_{inv,dis}$)must be considered in order to evaluate the actually available energy provided by the KERS.

$$f_{KERS} = \frac{E_{available}}{E_S} \bullet 100 = \frac{E_B \bullet \eta_{inv,dis}}{E_S} \bullet 100 \tag{17}$$

The environmental and economic benefits attainable by using the KERS to power a refrigeration unit in refrigerated transport applications are then evaluated by considering the primary energy savings (PES) and, consequently, the fuel savings (FS). The primary energy saved can be evaluated by considering that the electricity provided by the whole KERS (including the battery) would be otherwise produced by the thermal engine and converted into electricity by means of the auxiliary alternator, so the efficiency of the alternator (η_{alt}), of the thermal engine (η_{en}) and of the transmission (η_t) must be taken into account. In particular, a global efficiency η_g, given by the product between η_{alt}, η_{en} and η_t, is considered, so the primary energy saving can be calculated through the following equation.

$$PES = \frac{E_{available}}{\eta_g} \tag{18}$$

The calculation of the primary energy saving allows the evaluation of the fuel savings due to the KERS system, and consequently the attainable savings in environmental ($CO_{2,e}$ saving) and economic (cost saving) terms (Eqq. 19–21).

$$FS = \frac{PES}{LHV_{fuel}} \tag{19}$$

$$CO_{2,e}\ saving = FS \bullet \alpha_{fuel} \tag{20}$$

$$cost\ saving = FS \bullet c_{fuel} \tag{21}$$

where LHV_{fuel} is the lower heating value of the fuel considered, while α_{fuel} and c_{fuel} are its emission factor and unit cost.

3. Results and discussion

Given the van's speed during the delivery mission, the acceleration can be evaluated consequently. The vehicle is characterized by an aerodynamic resistance coefficient C_x of 0.316 (declared by the manufacturer), and a rolling friction coefficient C_r of $6.15 \cdot 10^{-3}$.

In order to explore the possibility of using an electric KERS to produce the electricity required by the refrigeration system, a specific commercial MGU has been considered, and the size has been selected based on the calculated braking power. The characteristic curve Torque-angular velocity implemented in the above-described model is shown in Fig. 4.

The MGU is supposed to be mechanically connected to the engine drive shaft via a fixed-ratio gear transmission, with a transmission ratio equal to 4.

The addition of the hybrid inverter, the battery and the MGU to the original system causes an increase in the vehicle weight, from 3499 kg to 3535 kg (about 1% increase).

Table 2 summarizes the characteristics of the whole system considered, including the vehicle, the specific MGU, the battery and the hybrid inverter.

The refrigeration system only operates during the delivery part of the mission (about 43 min, 20 km). Typically, the refrigerated van's cold room temperature is brought down to the desired level prior to beginning the delivery mission, so the test was performed considering these operating conditions after the pull-down phase.

As described in section 2.1., active and apparent electrical power have been measured during the delivery mission. A sample of the measurements performed during the test is shown in Fig. 5, where a single ON-OFF cycle is highlighted.

Measurements show that the VCR system requires about 842 Wh apparent electric energy (588 Wh active electrical energy), operating with a duty cycle equal to 0.56, in order to maintain a temperature of −10.1 °C inside the cold room, with a hysteretic behaviour between −7.8 °C and − 11.5 °C.

The numerical simulations aiming at estimating the electrical energy produced by the KERS during the delivery mission have been performed in Matlab/Simulink environment. Eqq. 5–15 have been solved at each time instant, with a time step of 1 s, in order to evaluate the braking

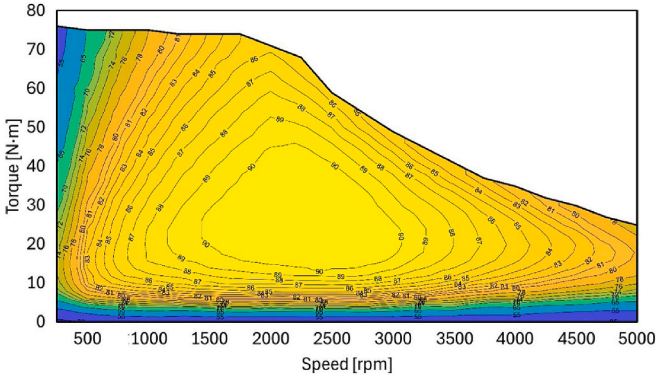

Fig. 4. Characteristic torque-angular velocity curve of the considered MGU.

Table 2
Characteristics of the hybrid refrigerated van.

Vehicle	Engine (F1CFA401A)	Four-stroke petrol-methane spark ignition Maximum power: 100 kW@ 2730–3500 rpm Maximum torque: 350 N · m @ 1500–2730 rpm Displacement: 2998 cm^3
	Drive type	Rear-wheel
	Weight	3499 kg (without KERS) 3535 kg (with KERS)
	C_x	0.316
	C_r	$6.15 \cdot 10^{-3}$
	Wheel radius	0.675 m
	Refrigeration system	Refrigerant: R452A Compressor: hermetic with inverter (30–80 Hz) Power supply: electricity grid or dedicated alternator
	Cold room	Reinforced isothermal class F Thermal transmittance (by ATP): 0.29 $Wm^{-1} K^{-1}$ Minimum temperature: −20 °C
MGU	Brand/model	MOTENERGY/ ME1507
	Weight	21.4 kg
	Stall torque	76 N · m
	Peak current	600 A
	Max speed	8000 rpm
	Declared efficiency	92%
	Inertia	960 kg · cm^2
	Cost	1065 €
Battery	Type	$LiFePO_4$
	Nominal Capacity	3600 Wh
	Nominal voltage	48 V
	Max. charge/ discharge current	150 A
	Cost	460.8 €
Hybrid inverter/ Power controller	Efficiency (charge) Efficiency (discharge)	93% [40]
	Cost	469 € [40]

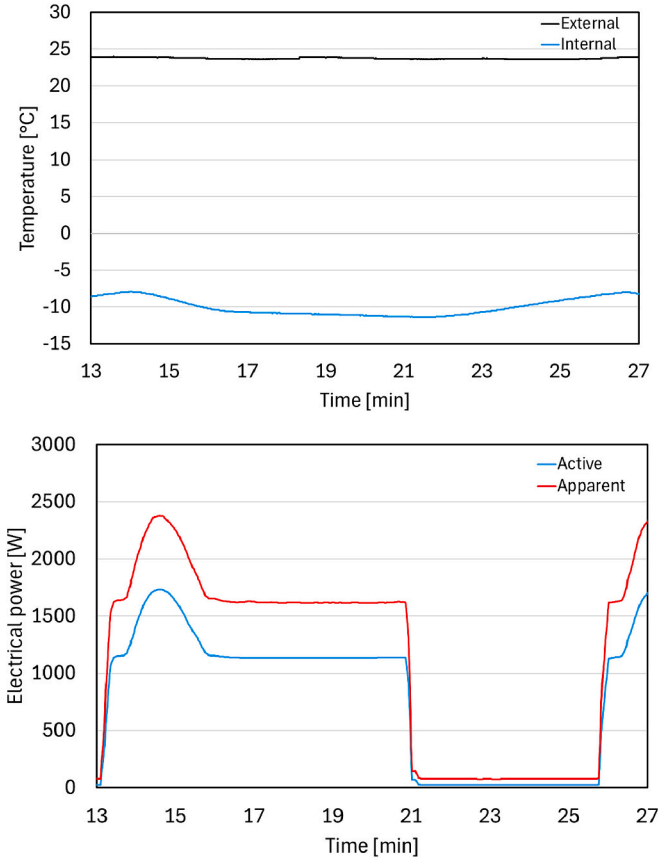

Fig. 5. Sample of temperature (top) and power (bottom) measurements performed during the experimental test.

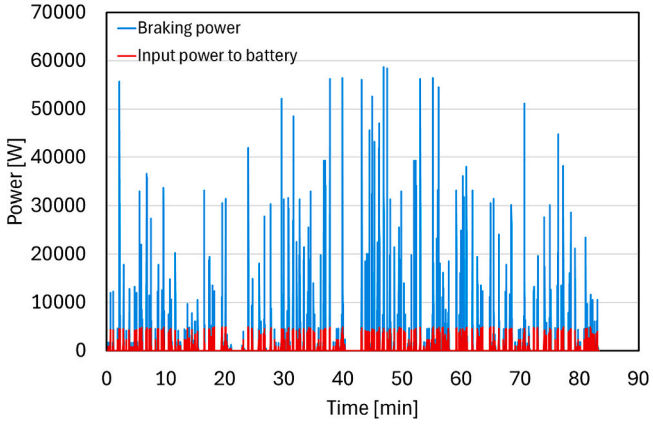

Fig. 6. Comparison between the braking power and the battery input power obtained by simulation.

power, first, and the power produced by the KERS, then, as described in Subsection 2.2. Fig. 6 shows the comparison between the braking power and the battery input electrical power. Fig. 7 shows the same comparison in terms of energies, including the MGU energy input.

Figs. 6 and 7 clearly show that the KERS system, including the inverter used to perform the AC/DC conversion, is able to convert only a portion of the braking/deceleration energy into electricity to be stored in the battery. The results obtained by simulation show that starting from a total breaking energy (mechanical) of 1746 Wh, only 717 Wh are made available to the MGU to be converted into electricity. In particular, an electrical energy of 429 Wh is stored in the battery, corresponding to 399 Wh of available electrical energy due to the inverter discharge efficiency.

In particular, an overall conversion efficiency, evaluated as the ratio between the battery input electrical energy and the total braking energy, of about 25% has been found. However, it is worth noting that the input power to the MGU, which is actually converted into electricity, is limited by several factors involving the motor-generator unit, but also the inverter and the battery as well, as described in Subsection 2.2. When considering the MGU input energy instead of the braking energy, the conversion efficiency is about 58%, since a non-negligible part of the braking energy cannot be converted into electricity.

The electricity demand coverage ratio (f_{KERS}) can be, therefore, evaluated by means of Eq. 16, obtaining that the use of the electric KERS, the inverter and the battery considered in this work, is able to provide 47.3% of the total electricity demand to power the refrigeration unit, showing a great potential in reducing the reliance on the thermal engine. Since the refrigeration unit contributes about 11.4% to the vehicle's total fuel consumption (Appendix A), the use of an electric KERS to power the VCR system could provide a reduction in the refrigerated vehicle fuel consumption of about 5.4%. This result is coherent with those obtained by BMW Efficient Dynamics (between 1% and 5%), which is the only commercial example of the use of electric KERS in internal combustion vehicles.

A 47.3% reduction in the electricity demand directly leads to the same reduction in fuel consumption and, consequently, in GHG emissions and costs. In order to evaluate primary energy, fuel and economic savings by means of Eqq. 16 and 17, the definition of η_g is needed (see Appendix A). The average (nominal), minimum and maximum values of the global efficiency used in the simulation phase are 23.0%, 18.3% and 27.2%, respectively.

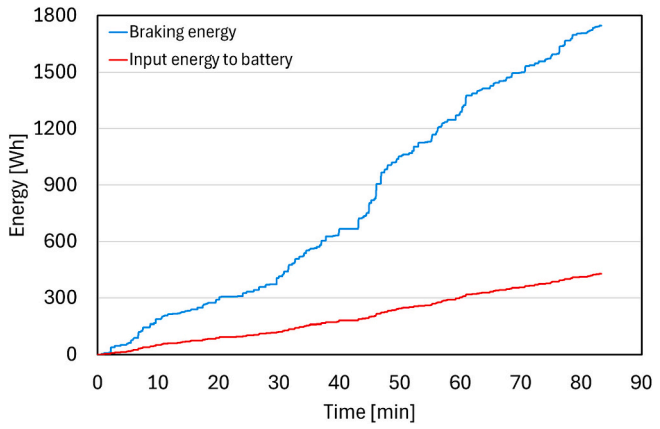

Fig. 7. Comparison between braking energy and battery input energy obtained by simulation.

In this specific case, the thermal engine is fuelled with methane, characterized by a LHV_{fuel} of 50 MJ/kg, an emission factor α_{fuel} of 0.244 $kgCO_{2,e}$/kWh and a unit cost c_{fuel} equal to 1.667 €/kg. Considering minimum ($\eta_{g,min}$), maximum ($\eta_{g,max}$) and nominal ($\eta_{g,nom}$) values of η_g, the results in terms of PES, FS, $CO_{2,e}$ and cost savings are reported in Table 3. Since the emission and economic savings are strictly related to the specific path in terms of distance and duration, savings per travelled kilometer are also evaluated.

As previously underlined, the results obtained correspond to 47.3% economic and emission savings, since they are proportional to the energy saved. It is important to mention that this work focuses on a short distance delivery mission, with the delivery location being only 20 km away from the depot. However, the results in terms of € per kilometer and $KgCO_{2,e}$ per kilometer are promising, considering the fact that refrigerated vans and trucks are usually employed for longer paths.

In order to estimate the payback period related to the implementation of the proposed KERS, the estimated cost savings have been used. The cost of the whole KERS is about €1995 (see costs in Table 2), while annual cost savings have been obtained by taking into account 5 working days per week and 50 weeks per year. A daily distance travelled of 200 km is considered, with 100 km for delivery and 100 km for the return to the depot. In these conditions, annual cost savings in the range 220–330 €/year have been found, resulting in a payback period of about 6–9 years, depending on the global efficiency value. When considering the average value of η_g, the payback period is equal to 8 years, meaning that the economic benefits provided by the proposed KERS would balance the cost of the system after 8 years.

It is worth noting that the KERS technology has the ability to fulfil nearly 50% of the refrigeration unit's electricity needs. Annual $CO_{2,e}$ savings in the range 451–671 $kg_{CO2,e}$ have been found, resulting in 4515–6710 $kg_{CO2,e}$ saved in a 10 years useful life for a refrigerated van. This demonstrates the potential for KERS to make a significant contribution towards decarbonization in the automotive industry, specifically in refrigerated transport applications.

It is worth noting that the results obtained in this study refer to specific working conditions (outdoor and set-point temperatures, irradiance conditions, wind speed, humidity, etc.), vehicle (model, weight, walls color, braking system, wheels) and refrigeration unit (plant and refrigerant). In order to obtain more general results, an experimental campaign is needed, considering different operating conditions, vehicles and refrigeration units. Moreover, it should be noted that this analysis does not represent the best possible scenario. However, with proper design optimization, the cost of each component can be reduced, thus increasing the attainable emission and cost savings, and reducing the payback period.

Table 3
Economic and emission savings.

	PES [Wh]	FS [kg]	$CO_{2,e}$ saving		Cost saving	
			[$kg_{CO2,e}$]	[$kg_{CO2,e}$/km]	[€]	[€/km]
$\eta_{g.min}$	2178	0.157	0.532	0.013	0.261	0.007
$\eta_{g,nom}$	1733	0.125	0.423	0.011	0.208	0.005
$\eta_{g,max}$	1465	0.106	0.358	0.009	0.176	0.004

4. Conclusions

The refrigerated transportation industry and the entire cold chain need to transition sustainably to reduce their environmental impact. Many solutions today focus on electrification across various sectors, particularly in the automotive industry, where onboard batteries are being incorporated. In this work, a kinetic energy recovery system is proposed for the application in refrigerated transport. The system is designed to recover the energy produced when the vehicle brakes or decelerates. This energy is then converted into electrical energy and stored in a $LiFePO_4$ battery. The stored energy can then be used to power an all-electric vapor compression refrigeration system, reducing the power demand to the internal combustion engine.

The KERS system's design prioritized minimal increase in vehicle mass and utilized commercially available components such as the Motor-Generator Unit, inverter, and battery. The MGU was chosen based on the maximum input power allowed, which corresponds to the highest breaking power achieved during an actual urban delivery task. As a result, a slight increase of about 1% in the vehicle mass has been found.

The estimation of the KERS electricity demand coverage ratio has been performed by considering data obtained from a real urban delivery mission, characterized by a duration of about 80 min and a distance of 40 km, performed in May 2023. This experimental test has allowed to obtain a genuine driving cycle by using an OBD scanner. Additionally, temperatures and energy consumption related to the operation of the VCR system have been measured. The results obtained show that the proposed KERS can provide more than 47% of the total electricity demand to power the refrigeration unit, corresponding to about a 5.4% reduction in the vehicle fuel consumption and therefore showing a great potential in reducing the reliance on the thermal engine. In the specific refrigerated van considered in this work, the refrigeration unit is powered by means of an alternator, which is directly driven by the thermal engine. This means that a 47.3% reduction in the energy consumption corresponds to a 47.3% reduction in fuel consumption for refrigeration purpose at the same operating conditions, resulting in 0.30–0.48 $KgCO_{2,e}$ emissions avoided and an economic saving of 17–25 c€.

In addition to these results, which are strictly dependent on the mission considered in terms of distance and duration, emission and cost savings per travelled kilometer have been evaluated. In particular, emission savings of 0.008–0.012 $kgCO_{2,e}$/km and cost savings of 0.004–0.006 €/km have been found. These results are ideal for analyzing a typical urban driving cycle that includes random acceleration and deceleration phases. For a generic 200 km daily operation of a refrigerated van in urban context, annual savings have been estimated, obtaining a payback period related to the implementation of the KERS in the range 6–9 years. In addition, considering a useful life equal to 10 years for a refrigerated van, 4515–6710 $kg_{CO2,e}$ could be saved.

The use of hybrid refrigerated vans can significantly reduce carbon emissions in the cold chain. However, it is essential to carefully consider their design to ensure optimal performance, as high investment costs may hinder the adoption of these environmentally-friendly systems. This study has analyzed the potential of using a KERS for refrigerated transportation and found promising results. In order to achieve maximum efficiency and cost-effectiveness, it is crucial to optimize all components of the system while considering economic and energy factors.

Therefore, future works should focus on testing alternative scenarios with varying operating conditions and technology adoption. This will

help optimize the design of the entire KERS system and provide a comprehensive understanding of the potential savings that can be achieved through this kind of refrigerated van hybridization. The natural evolution of this study is of course the implementation of an electric KERS on a refrigerated van equipped with a VCR unit, in order to experimentally verify the actual fuel, emissions and cost savings. Moreover, the environmental impact of this technology should be addressed by considering the entire cold chain. In addition, the coupling of the proposed electric KERS with a photovoltaic system placed on the rooftop of the refrigerated vehicle, should be investigated.

Funding

This research did not receive any specific grant from funding agencies in the public, commercial, or not-for-profit sectors.

CRediT authorship contribution statement

Angelo Maiorino: Supervision, Methodology, Investigation, Conceptualization. **Fabio Petruzziello:** Writing – review & editing, Writing – original draft, Investigation, Data curation. **Arcangelo Grilletto:** Writing – review & editing, Writing – original draft, Investigation, Data curation. **Ciro Aprea:** Supervision, Methodology, Investigation, Conceptualization.

Declaration of competing interest

The authors declare no conflict of interest.

Data availability

We have uploaded supplementary materials in .csv format, including the data used to perform the numerical analysis, the simulation results and the data presented in Appendix A

Appendix A

Transport refrigeration units can be powered by means of an auxiliary alternator mechanically connected to the thermal engine by means of a pulley and belt transmission system [34]. In this configuration, the alternator can produce electricity to power the VCR unit's compressor. This electricity production is performed starting from the fuel combustion in the thermal engine, so a series of efficiencies can be identified. In particular, the primary energy from fuel combustion is converted into mechanical work by the thermal engine, exhibiting an efficiency η_{en}. This mechanical work is transmitted to the auxiliary alternator by means of a pulley and belt transmission system with an efficiency given by η_t, and then converted into electricity by the alternator, which is characterized by an efficiency η_{alt}. Since the aim is to evaluate the link between the primary energy and the electricity produced, the authors defined and performed an experimental campaign to evaluate a global efficiency η_g given by the product between η_{en}, η_t and η_{alt}.

For testing purposes, an urban path simulating a generic multi-delivery mission has been defined. Three experimental tests have been performed with the VCR system turned off, with the aim of evaluating the fuel consumption of the van for traction only. Three other tests have been performed with the VCR unit turned on, in order to evaluate the total fuel consumption, including both traction and refrigeration contributions. Fuel consumption and the van's speed during the path have been recorded by means of an OBD scanner. The data obtained in traction-only and traction/refrigeration operating conditions are shown in Fig. A.1 and A.2, respectively.

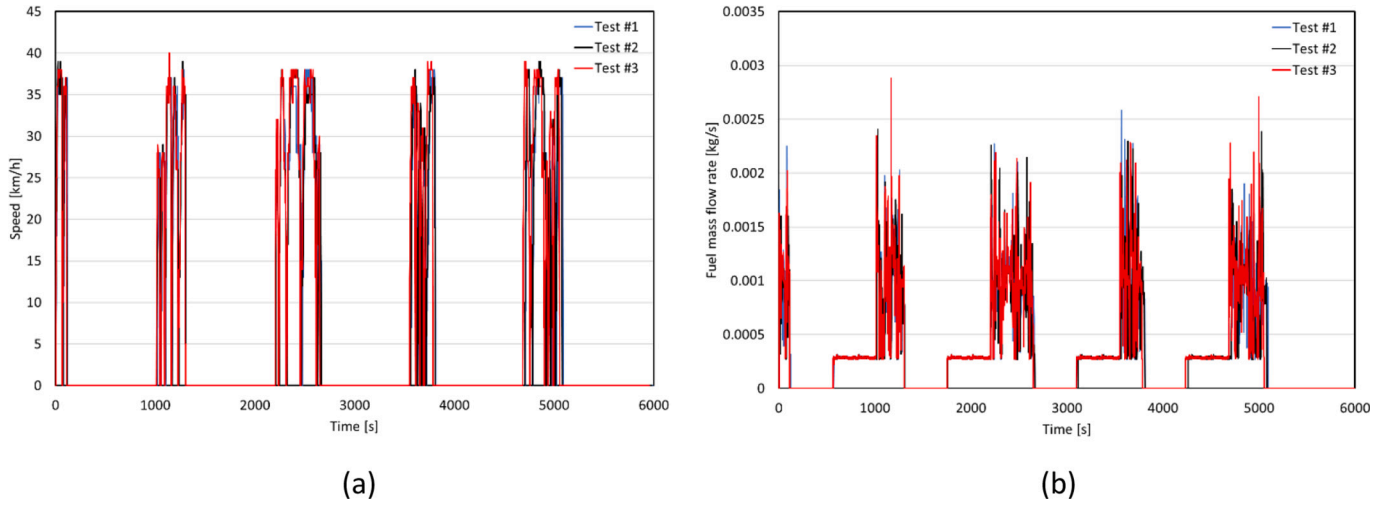

Fig. A.1. Data recorded in traction-only tests: (a) van's speed; (b) fuel consumption.

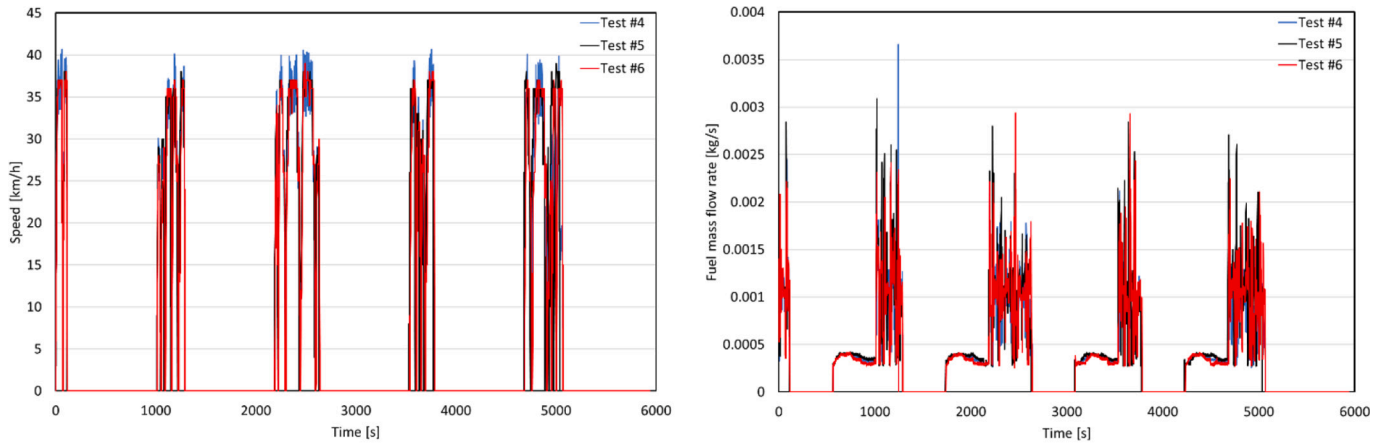

Fig. A.2. Data recorded in traction/refrigeration tests: (a) van's speed; (b) fuel consumption.

Table A.1 summarizes the characteristics of the path considered and the data recorded during the six tests.

Table A1
Data recorded during the experimental tests.

	Traction only			Traction/Refrigeration		
	Test #1	Test #2	Test #3	Test #4	Test #5	Test #6
Distance [km]	10.96	10.93	10.94	10.93	10.95	10.89
Duration [min]	99.8	99.7	99.2	99.5	98.9	99.5
Max speed [km/h]	38	39	40	40.7	39	39
Number of deliveries [−]	5					
Delivery duration (each) [min]	15					
Idling time [min]	30					
Vehicle off-time [min]	45					
VCR system on-time [min]	–	–	–	44.5	43.9	44.5
Fuel consumption [kg]	1.899	1.893	1.947	2.148	2.194	2.131
Primary energy [kWh]	26.4	26.3	27.0	29.8	30.4	29.6
Electricity consumption [Wh]	–	–	–	751	896	697

The amount of fuel used to power the VCR system ($m_{fuel,ref}$) can be evaluated by solving Eq. (A.1).

$$m_{fuel,ref} = m_{fuel,tot} - m_{fuel,traction} \tag{A.1}$$

where $m_{fuel,tot}$ is the fuel consumption related to traction/refrigeration operating mode, while $m_{fuel,traction}$ is the one related to traction-only conditions. Starting from the data recorded during the experimental tests, results show that the VCR unit contributes about 11.3% to the vehicle's total fuel consumption.

As shown in Table A.1, during the refrigeration/traction tests, the electricity consumption related to the VCR system operation has been measured by means of an energy meter characterized by a declared accuracy of ±0.7% of measured value. The global efficiency η_g can be, therefore, evaluated by solving Eq. (A.2).

$$\eta_g = \frac{Electricity\ consumption}{Primary\ energy\ for\ refrigeration} \tag{A.2}$$

Results have shown a global efficiency ranging between 18.3% and 27.2%, with an average value of 23.3%.

Appendix B. Supplementary data

Supplementary data to this article can be found online at https://doi.org/10.1016/j.apenergy.2024.123145.

References

[1] L. DJ. The Role of Refrigeration in the Global Economy. In: 38th Note on Refrigeration Technologies. 2019; 2019.
[2] She X, Cong L, Nie B, Leng G, Peng H, Chen Y, et al. Energy-efficient and -economic technologies for air conditioning with vapor compression refrigeration: a comprehensive review. Appl Energy 2018;232:157–86. https://doi.org/10.1016/j.apenergy.2018.09.067.
[3] Koronaki IP, Cowan D, Maidment G, Beerman K, Schreurs M, Kaar K, et al. Refrigerant emissions and leakage prevention across Europe – results from the RealSkillsEurope project. Energy 2012;45:71–80. https://doi.org/10.1016/j.energy.2012.05.040.
[4] Tassou SA, Grace IN. Fault diagnosis and refrigerant leak detection in vapour compression refrigeration systems. Int J Refrigerat 2005;28:680–8. https://doi.org/10.1016/j.ijrefrig.2004.12.007.
[5] Alsouda F, Bennett NS, Saha SC, Salehi F, Islam MS. Vapor compression cycle: a state-of-the-art review on cycle improvements, water and other natural

refrigerants. Clean Technol 2023;5:584–608. https://doi.org/10.3390/cleantechnol5020030.
[6] Su P, Ji J, Cai J, Gao Y, Han K. Dynamic simulation and experimental study of a variable speed photovoltaic DC refrigerator. Renew Energy 2020;152:155–64. https://doi.org/10.1016/j.renene.2020.01.047.
[7] Alrwashdeh SS, Ammari H. Life cycle cost analysis of two different refrigeration systems powered by solar energy. Case Stud Therm Eng 2019;16:100559. https://doi.org/10.1016/j.csite.2019.100559.
[8] Lazzarin RM, Noro M. Past, present, future of solar cooling: technical and economical considerations. Solar Energy 2018;172:2–13. https://doi.org/10.1016/j.solener.2017.12.055.
[9] Opoku R, Anane S, Edwin IA, Adaramola MS, Seidu R. Comparative techno-economic assessment of a converted DC refrigerator and a conventional AC refrigerator both powered by solar PV. Int J Refrigerat 2016;72:1–11. https://doi.org/10.1016/j.ijrefrig.2016.08.014.
[10] Salilih EM, Birhane YT. Modelling and performance analysis of directly coupled vapor compression solar refrigeration system. Solar Energy 2019;190:228–38. https://doi.org/10.1016/j.solener.2019.08.017.
[11] Yıldız G, Gürel AE, Ceylan İ, Ergün A, Karaağaç MO, Ağbulut Ü. Thermodynamic analyses of a novel hybrid photovoltaic-thermal (PV/T) module assisted vapor compression refrigeration system. J Build Eng 2023;64:105621. https://doi.org/10.1016/j.jobe.2022.105621.
[12] Zarei A, Liravi M, Rabiee MB, Ghodrat M. A novel, eco-friendly combined solar cooling and heating system, powered by hybrid photovoltaic thermal (PVT) collector for domestic application. Energ Conver Manage 2020;222:113198. https://doi.org/10.1016/j.enconman.2020.113198.
[13] UNEP. 2010 Report of the Refrigeration, Air Conditioning and Heat Pumps Technical Options Committee 2010 Assessment. 2024.
[14] Automotive Fleet. Environmental Danger of Global Refrigerated Transport Studied. 2015. Accessed on 01.08.2023 2015.
[15] Mehra A. Refrigerated Transport Market by Application (Chilled food & Frozen food), Mode of Transport (Road, Sea, Rail & Air), Vehicle Type (LCV, MHCV & HCV), Temperature (Single & Multi-temperature), Technology and Region - Global Forecast to 2027. https://wwwmarketsandmarketscom/market-reports/refrigerated-transport-market-779494html; 2022 (Accessed February 7, 2024) n.d.
[16] de Micheaux TL, Ducoulombier M, Moureh J, Sartre V, Bonjour J. Experimental and numerical investigation of the infiltration heat load during the opening of a refrigerated truck body. Int J Refrigerat 2015;54:170–89. https://doi.org/10.1016/j.ijrefrig.2015.02.009.
[17] Tassou SA, De-Lille G, Ge YT. Food transport refrigeration – approaches to reduce energy consumption and environmental impacts of road transport. Appl Therm Eng 2009;29:1467–77. https://doi.org/10.1016/j.applthermaleng.2008.06.027.
[18] Yang Z, Tate JE, Morganti E, Shepherd SP. Real-world CO2 and NOX emissions from refrigerated vans. Sci Total Environ 2021;763:142974. https://doi.org/10.1016/j.scitotenv.2020.142974.
[19] Maiorino A, Petruzziello F, Aprea C. Refrigerated transport: state of the art, technical issues. Innov Chall Sustain Energ (Basel) 2021;14:7237. https://doi.org/10.3390/en14217237.
[20] Le TT, Sharma P, Bora BJ, Tran VD, Truong TH, Le HC, et al. Fueling the future: a comprehensive review of hydrogen energy systems and their challenges. Int J Hydrogen Energy 2024;54:791–816. https://doi.org/10.1016/j.ijhydene.2023.08.044.
[21] Kougias I, Taylor N, Kakoulaki G, Jäger-Waldau A. The role of photovoltaics for the European green Deal and the recovery plan. Renew Sustain Energy Rev 2021;144:111017. https://doi.org/10.1016/j.rser.2021.111017.
[22] Council of the EU R. The European Council. Fit for 55. from, https://www.consilium.europa.eu/en/policies/green-deal/fit-for-55-the-eu-plan-for-a-green-transition/; 2023.
[23] Bakır H, Ağbulut Ü, Gürel AE, Yıldız G, Güvenç U, Soudagar MEM, et al. Forecasting of future greenhouse gas emission trajectory for India using energy and economic indexes with various metaheuristic algorithms. J Clean Prod 2022:360. https://doi.org/10.1016/j.jclepro.2022.131946.
[24] Zhang Y, Li K, Cui S, Sun Y. Power distribution strategy for an electric bus with a hybrid energy storage system. World Electric Vehicle J 2021;12:154. https://doi.org/10.3390/wevj12030154.
[25] Xiao B, Ruan J, Yang W, Walker PD, Zhang N. A review of pivotal energy management strategies for extended range electric vehicles. Renew Sustain Energy Rev 2021;149:111194. https://doi.org/10.1016/j.rser.2021.111194.
[26] Ren G, Ma G, Cong N. Review of electrical energy storage system for vehicular applications. Renew Sustain Energy Rev 2015;41:225–36. https://doi.org/10.1016/j.rser.2014.08.003.
[27] Tchobansky L, Kozek M, Schlager G, Jörgl HP. A purely mechanical energy storing concept for hybrid vehicles. In: SAE Technical Papers. SAE International; 2003. https://doi.org/10.4271/2003-01-3278.
[28] Barr A, Veshagh A. Fuel economy and performance comparison of alternative mechanical hybrid powertrain. Configurations 2008. https://doi.org/10.4271/2008-01-0083.
[29] Gabriel-Buenaventura A, Azzopardi B. Energy recovery systems for retrofitting in internal combustion engine vehicles: a review of techniques. Renew Sustain Energy Rev 2015;41:955–64. https://doi.org/10.1016/j.rser.2014.08.083.
[30] BMW Efficient Dynamics - Less Fuel Consumption. More driving pleasure. Retrieved at, https://www.bmw-lao.la/en/topics/fascination-bmw/efficient-dynamics/overview.html; 2024.
[31] Kumar NS. Increasing the cruise range and reducing the capital cost of electric vehicles by integrating auxiliary unit with the traction drive. Int J Vehicul Technol 2016;2016:1–11. https://doi.org/10.1155/2016/7617692.
[32] Zhang Y, Tong L. Regenerative braking-based hierarchical model predictive cabin thermal management for battery life extension of autonomous electric vehicles. J Energy Storage 2022;52:104662. https://doi.org/10.1016/j.est.2022.104662.
[33] Hamada AT, Orhan MF. An overview of regenerative braking systems. J Energy Storage 2022;52:105033. https://doi.org/10.1016/j.est.2022.105033.
[34] Tassou SA, De-Lille G, Ge YT. Food transport refrigeration – approaches to reduce energy consumption and environmental impacts of road transport. Appl Therm Eng 2009;29:1467–77. https://doi.org/10.1016/j.applthermaleng.2008.06.027.
[35] Maiorino A, Mota-Babiloni A, Petruzziello F, Del Duca MG, Ariano A, Aprea C. A comprehensive energy model for an optimal design of a hybrid refrigerated van. Energies (Basel) 2022;15:4864. https://doi.org/10.3390/en15134864.
[36] Pipitone E, Vitale G. A regenerative braking system for internal combustion engine vehicles using supercapacitors as energy storage elements - Part 1: system analysis and modelling. J Power Sources 2020;448:227368. https://doi.org/10.1016/j.jpowsour.2019.227368.
[37] Sharma P, Bora BJ. A review of modern machine learning techniques in the prediction of remaining useful life of Lithium-ion batteries. Batteries 2023:9. https://doi.org/10.3390/batteries9010013.
[38] Xu Y, Zhang B, Ge Z, Zhang S, Song B, Tian Y, et al. Advances and perspectives towards spent LiFePO4 battery recycling. J Clean Prod 2024;434:140077. https://doi.org/10.1016/j.jclepro.2023.140077.
[39] Maiorino A, Cilenti C, Petruzziello F, Aprea C. A review on thermal management of battery packs for electric vehicles. Appl Therm Eng 2024;238:122035. https://doi.org/10.1016/j.applthermaleng.2023.122035.
[40] Pipitone E, Vitale G, Lanzafame R, Brusca S, Mauro S, Beccari S. A feasibility analysis of an electric KERS for internal combustion engine vehicles. In: SAE Technical Papers. SAE International; 2019. https://doi.org/10.4271/2019-24-0241.